Phonon Dispersion and the Competition between Pairing and Charge Order

N. C. Costa,[1,2,*] T. Blommel,[2,3] W.-T. Chiu,[2] G. Batrouni,[4,5] and R. T. Scalettar[2]

[1]*Instituto de Física, Universidade Federal do Rio de Janeiro, Cx.P. 68.528, 21941-972 Rio de Janeiro RJ, Brazil*
[2]*Department of Physics, University of California, Davis, California 95616, USA*
[3]*Department of Physics, North Dakota State University, Fargo, North Dakota 58105, USA*
[4]*Université Côte d'Azur, INPHYNI, CNRS, 0600 Nice, France*
[5]*Beijing Computational Science Research Center, Beijing 100193, China*

The Holstein model describes the interaction between fermions and a collection of local (dispersionless) phonon modes. In the dilute limit, the phonon degrees of freedom dress the fermions, giving rise to polaron and bipolaron formation. At higher densities, the phonons mediate collective superconducting (SC) and charge-density wave (CDW) phases. Quantum Monte Carlo (QMC) simulations have considered both these limits but have not yet focused on the physics of more general phonon spectra. Here we report QMC studies of the role of phonon dispersion on SC and CDW order in such models. We quantify the effect of finite phonon bandwidth and curvature on the critical temperature T_{cdw} for CDW order and also uncover several novel features of diagonal long-range order in the phase diagram, including a competition between charge patterns at momenta $\mathbf{q} = (\pi, \pi)$ and $\mathbf{q} = (0, \pi)$ which lends insight into the relationship between Fermi surface nesting and the wave vector at which charge order occurs. We also demonstrate SC order at half filling in situations where a nonzero bandwidth sufficiently suppresses T_{cdw}.

Introduction.—Monte Carlo (QMC) methods have evolved into a powerful tool to understand the physics of strongly interacting quantum systems. Nevertheless, many qualitative questions remain largely unaddressed concerning electron-phonon models. One of the most prominent concerns is the origin of charge-density wave (CDW) formation, especially in dimensions greater than one. Increasingly, attention has turned to alternatives to the original Peierls picture [1]. Zhu *et al.* [2,3] have proposed at least three classes of CDWs: (i) those associated with the Peierls instability and Fermi surface nesting (FSN), typically in quasi-1D materials; (ii) those driven by a momentum-dependent electron-phonon coupling (EPC) $g_{\mathbf{q}}$, such as the quasi-2D material $NbSe_2$ [2,4–9], for which a CDW phase sets in at $T_{cdw} = 33.5$ K, even though angle-resolved photoemission spectroscopy measurements do not show any sign of FSN [2]; and (iii) systems where electron correlations may drive to charge modulation, a primary example being the cuprates [10]. In addition to CDW physics, closely related current issues in (high-temperature) superconductivity (SC) also invite a return to the study of electron-phonon interactions. For instance, a momentum-dependent EPC is believed to be implicated in the dramatic increase in the superconducting transition temperature T_{sc} of FeSe monolayers on $SrTiO_2$ [11–13].

The random phase approximation (RPA) criterion, $4g_{\mathbf{q}}^2/\omega(\mathbf{q}) > 1/\chi_0(\mathbf{q})$, where $\chi_0(\mathbf{q})$ is the bare electronic susceptibility, suggests that the shape of the bare phonon dispersion, $\omega(\mathbf{q})$, should affect charge ordering and hence be important to the analysis of the above-mentioned second type of CDW. In view of this, here we explore a new scenario in which phonon dispersion plays a primary role in determining the CDW ordering wave vector and critical temperature and where SC can supplant diagonal long-range order. We extend QMC simulations [14] of a 2D square lattice Holstein model (HM) to include phonon dispersion [15–17]. For the HM on a bipartite lattice, CDW order dominates over SC at commensurate fillings, similarly to the dominance of antiferromagnetism over pairing at half filling in the Hubbard Hamiltonian [27,28]. In that model, it is known [29] that off-diagonal long-range order (ODLRO) can be made more competitive by adjusting the fermionic dispersion relation, e.g., by introducing a next-nearest-neighbor hopping t', or via doping. Both of these serve to destroy the perfect nesting of the square lattice Fermi surface. Here we adopt a different approach, which is available in an electron-phonon model—tuning the phonon dispersion while retaining the features of the bare electronic Fermi surface, i.e., its FSN. The relevance of this approach can be inferred by its effects on polaron formation, as showed in a recent studies [16]. We examine in this Letter the many-electron problem, with our results supporting the picture that the shape of the phonon dispersion plays an important role in the CDW (or SC) formation, i.e., being responsible for enhancing or suppressing it. It is worth noting that CDW formation can also be motivated at strong coupling: Large g causes pair formation, and then $t^2/(g^2/\omega)$ provides an additional energy lowering when
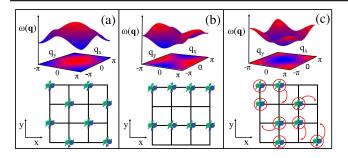
FIG. 1. Sketch of bare phonon dispersion (top) and its resulting charge ordering (bottom) for (a) downward curvature, (b) mixed curvature (saddle point at the origin), and (c) upward curvature cases. The arrows on the latter correspond to the (possible) hopping to any available sites and emphasize the possibility of mobile pairs.

doubly occupied and empty sites alternate. This is the analog of the strong coupling picture of AFM order in the Hubbard model, where the exchange energy $J \sim t^2/U$ favors adjacent spins which are antiparallel.

Figure 1 presents the qualitative pictures behind our key results: Bare phonon dispersion with (a) a downward curvature in going from $\mathbf{q} = (0,0)$ to $\mathbf{q} = (\pm\pi, \pm\pi)$ leads to an enhancement of the CDW gap and increases T_{cdw} at half filling; (b) a mixed curvature (saddle point at the origin, i.e., upward in $\hat{x}$ and downward in $\hat{y}$ directions) can lead to striped charge order—further emphasizing that charge order and FSN wave vectors do not have to be identical; and (c) an upward curvature, which suppresses the CDW gap and, for a sufficiently large bandwidth, can drive a CDW-SC transition at *commensurate filling*. We emphasize that, in what follows, the dispersion will be relatively small, far from the limit of introducing a zero-energy phonon mode which would trivially lead to CDW formation. A weak curvature in the phonon dispersion can shift the CDW wave vector away from the FSN vector and even replace CDW order by superconductivity.

Methodology.—The Holstein model [30]

$$\mathcal{H}_1 = -t \sum_{\langle \mathbf{i,j}\rangle,\sigma} (d^\dagger_{\mathbf{i}\sigma} d_{\mathbf{j}\sigma} + \text{H.c.}) - \mu \sum_{\mathbf{i},\sigma} n_{\mathbf{i},\sigma}$$
$$+ \lambda \sum_{\mathbf{i},\sigma} n_{\mathbf{i},\sigma} \hat{X}_{\mathbf{i}} + \frac{1}{2}\sum_{\mathbf{i}} \hat{P}_{\mathbf{i}}^2 + \frac{\omega_1^2}{2}\sum_{\mathbf{i}} \hat{X}_{\mathbf{i}}^2 \quad (1)$$

is one of the simplest tight-binding descriptions of the electron-phonon interaction. A single electronic band, with fermionic creation (destruction) operators at site $\mathbf{i}$, $d^\dagger_{\mathbf{i},\sigma}(d_{\mathbf{i},\sigma})$, couples to independent oscillator degrees of freedom $\hat{X}_{\mathbf{i}}, \hat{P}_{\mathbf{i}}$. We consider here a square lattice with periodic boundary conditions, nearest-neighbor (NN) electron hopping $t = 1$ (to set the scale of energy), chemical potential μ, electron-phonon coupling λ, and local phonon frequency ω_1.

We generalize Eq. (1) to $\mathcal{H} = \mathcal{H}_1 + \mathcal{H}_2$, to include a coupling of strength ω_2 between NN displacements $\hat{X}_{\mathbf{i}}$, $\hat{X}_{\mathbf{j}}$, with

$$\mathcal{H}_2 = \frac{\omega_2^2}{2} \sum_{\langle \mathbf{i,j}\rangle} (\hat{X}_{\mathbf{i}} \pm \hat{X}_{\mathbf{j}})^2. \quad (2)$$

We will allow for both signs of this intersite term, i.e., for cases where the sign between neighboring sites $\langle \mathbf{i}, \mathbf{j}\rangle$ in the $\hat{x}$ and $\hat{y}$ directions are equal or different. Physically, the minus sign is the more natural one: Forces on atoms depend on their relative displacement. On the other hand, as we discuss below, the positive sign yields a mode with a downward bending momentum 0 to π, the more typical behavior for high-frequency optical modes.

The inclusion of NN coupling $\omega_2 \neq 0$ leads to a finite phonon bandwidth $\Delta\omega$. In the absence of the electron-phonon coupling, the quadratic bosonic Hamiltonian can be solved exactly, leading to a bare phonon dispersion relation: $\omega(\mathbf{q}) = \sqrt{\omega_1^2 + 2\omega_2^2[2 \pm \cos(q_x) \pm \cos(q_y)]}$. Positive signs reduce $\omega(\pi,\pi)$, making it energetically less costly to create a phonon at the M point, while negative signs favor modes at the zone center Γ point, $\omega(0,0)$. A mixed sign breaks rotational symmetry, producing a phonon in the X (or X') point, $\omega(\pi,0)$ [or $\omega(0,\pi)$]. As depicted in Fig. 1, these three cases are considered in this Letter.

Our discussion will benefit from the introduction of the following dimensionless parameters: (i) the adiabaticity ratio $\omega_0/t \equiv \omega(0,0)/t$; (ii) the phonon bandwidth $\Delta\omega/\omega_0$, with $\Delta\omega \equiv \max[\omega(\mathbf{q})] - \min[\omega(\mathbf{q})]$; and (iii) the electron-phonon coupling

$$\lambda_D = \frac{1}{W}\frac{1}{N}\sum_{\mathbf{q}} \frac{\lambda^2}{\omega^2(\mathbf{q})}, \quad (3)$$

which is the polaron binding energy, in units of half electronic bandwidth. Here $N = L^2$ is the number of sites, while the electronic bandwidth is $W = 8t$. Through an appropriate particle-hole transformation and shift of the phonon origin, one can show that a half filled electronic band occurs at $\mu = -\lambda^2/\omega_0^2$, for any dispersion relation $\omega(\mathbf{q})$. We therefore introduce $\tilde{\mu} = \mu + \lambda^2/\omega_0^2$, so that $\rho = 1$ at $\tilde{\mu} = 0$. In what follows, the Hamiltonian parameters λ, ω_1, and ω_2 are adjusted in order to fix the dimensionless ratios, ω_0/t, $\Delta\omega/\omega_0$, and λ_D, with $\rho = 1$. We consider here $\omega_0/t = 1$, unless otherwise indicated, and only small values of $\Delta\omega/\omega_0$, so that the bare phonon dispersion retains its nearly flat, optical form.

We examine the features of this generalized HM using determinant quantum Monte Carlo (DQMC) method [18–21]; see Supplemental Material [17] for more details. The nature of charge ordering is investigated by the equal-time charge-density structure factor

$S(\mathbf{q}) = (1/N)\sum_{\mathbf{i},\mathbf{j}} e^{i\mathbf{q}\cdot(\mathbf{i}-\mathbf{j})}\langle n_{\mathbf{i}} n_{\mathbf{j}}\rangle$, while pairing features are analyzed by the s-wave superconducting pair susceptibility $P_s = (1/N)\int_0^\beta d\tau \langle \Delta(\tau)\Delta^\dagger(0) + \text{H.c.}\rangle$, with $\Delta(\tau) = \sum_{\mathbf{i}} c_{\mathbf{i}\downarrow}(\tau)c_{\mathbf{i}\uparrow}(\tau)$ [31].

Before presenting our main results on the effects of phonon dispersion on charge and pairing order, we revisited the dispersionless ($\omega_2 = 0$) HM. It is worth mentioning that only recently have accurate results for the critical temperature been obtained [32–34], with its precise determination being provided via finite size scaling. Since the HM exhibits a finite temperature phase transition with a discrete order parameter, this transition should be in the universality class of the 2D Ising model. Hence,

$$S(\pi,\pi) = L^{2-\eta} f[L(\beta - \beta_c)^\nu], \qquad (4)$$

with $\eta = 1/4$ and $\nu = 1$. For instance, fixing $\lambda_D = 0.25$, $\omega_0/t = 1$, at half filling, we estimate $\beta_c = 6.0 \pm 0.1$; see Supplemental Material [17]. This value of β_c is somewhat lower than the earliest DQMC results [20,24] but is in agreement with more recent simulations [32,33] and will be used as a benchmark when analyzing the effects of phonon dispersion.

Effect of dispersion on charge correlations.—We first consider the case in which Eq. (2) has the same sign for both spatial directions. A positive coupling $(\hat{X}_{\mathbf{i}} + \hat{X}_{\mathbf{j}})$ in Eq. (2) corresponds to $\omega(\pi,\pi) < \omega_0$ and is expected to enhance CDW order. On the other hand, a negative coupling leads to $\omega(\pi,\pi) > \omega_0$ and charge order at the M point. These two cases correspond to Figs. 1(a) and 1(c), respectively. We define $\Delta\omega = \omega(\pi,\pi) - \omega_0$, i.e., $\Delta\omega > 0$ (<0) for upward (downward) phonon dispersion. The effect of $\omega_2 \neq 0$ is quantified in Fig. 2, which shows the charge gap induced in $\rho(\tilde{\mu})$ by the electron-phonon coupling [35]. This CDW gap grows or shrinks with the phonon bandwidth, depending on the shape its dispersion, i.e., if it is downward or upward, respectively. As presented in the inset in Fig. 2, this behavior is accompanied by changes in $\beta_c = 1/T_{\text{cdw}}$, obtained by the scaling analysis of $S(\pi,\pi)$ using Eq. (4); see, e.g., Supplemental Material [17]. It is remarkable that T_{cdw} can decrease by a factor of 2 with a relatively small $\Delta\omega/\omega_0 \approx 0.1$.

A mixed sign, in which the phonon dispersion terms in Eq. (2) take the form $\hat{X}_{\mathbf{i}} - \hat{X}_{\mathbf{j}}$ for $\mathbf{j} = \mathbf{i} + \hat{x}$ and $\hat{X}_{\mathbf{i}} + \hat{X}_{\mathbf{j}}$ for $\mathbf{j} = \mathbf{i} + \hat{y}$, results in a phonon spectrum with a saddle point at $\mathbf{q} = (0,0)$, with minima at $\mathbf{q} = (0,\pm\pi)$ and maxima at $\mathbf{q} = (\pm\pi, 0)$; see, e.g., Fig. 1(b). Figure 3 shows the charge structure factors for checkerboard [$\mathbf{q} = (\pi,\pi)$] and striped [$\mathbf{q} = (0,\pi)$] order as a function of the phonon bandwidth $\Delta\omega = \omega(\pi,0) - \omega(0,\pi)$, for fixed $\lambda_D = 0.25$, $\omega_0/t = 1$, $\beta = 10$, and $L = 8$. In contrast to the case of identical signs, for which a small $\Delta\omega/\omega_0 \sim 0.1$ had a large effect on the gap and T_{cdw}, charge correlations here are initially almost independent of $\Delta\omega$ up to $\Delta\omega/\omega_0 \sim 0.25$. However,
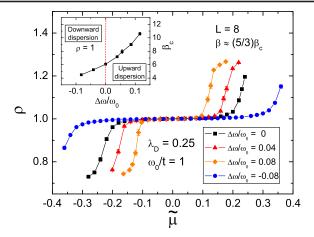

FIG. 2. Dependence of electronic density ρ on chemical potential $\tilde{\mu}$, fixing $\lambda_D = 0.25$, $\omega_0/t = 1$, and $\Delta\omega/\omega_0 = 0$ (black squares), 0.04 (red triangles), 0.08 (orange diamonds), and -0.08 (blue circles). The energy scale is fixed for all cases, with $\beta \approx \frac{5}{3}\beta_c$ (i.e., $\beta = 10$, 12, 15, and 8, respectively). Negative and positive signs for the bandwidth $\Delta\omega$ correspond to $\omega(\pi,\pi) < \omega_0$ and $\omega(\pi,\pi) > \omega_0$, respectively. Inset: Inverse critical temperature as a function of $\Delta\omega$. Here, and in all subsequent figures, when not shown, error bars are smaller than the symbol size.

at $\Delta\omega/\omega_0 \sim 0.30$ a strong suppression of $S(\pi,\pi)$ occurs, with a corresponding rapid rise in $S(0,\pi)$. This transition point is almost independent of ω_0/t, as displayed in Fig. 3 (inset). It is expected that this phase transition would be first order, due to different symmetries associated to the ground states. One should notice that the bare fermion dispersion relation is of course *independent* of $\Delta\omega$; i.e., it retains the nesting at (π,π) and the van Hove singularity at $\rho = 1$. The onset of striped charge order is driven by changes in the phonon dispersion, not by changes in the FSN.
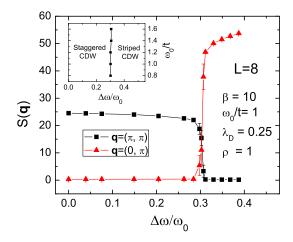

FIG. 3. CDW structure factor as a function of the phonon bandwidth for the mixed curvature dispersion case, i.e., upward in $\hat{x}$ and downward in $\hat{y}$ directions. A phase transition from staggered to striped order occurs at around $\Delta\omega/\omega_0 = 0.30$, independent of ω_0/t (inset).
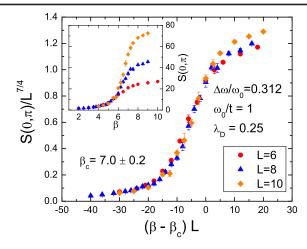
FIG. 4. Data collapse of the DQMC results of $S(0, \pi)$ for the mixed curvature (saddle point) case, fixing the 2D Ising critical exponents. Inset: Charge structure factor as a function of β. Here $\Delta\omega/\omega_0 = 0.312$.

We can also obtain the transition temperature for the striped phase. The inset in Fig. 4 shows raw data for $S(0, \pi)$ on different lattice sizes as a function of β, for $\Delta\omega/\omega_0 = 0.312$, slightly after entering into the striped phase. The corresponding scaling (data collapse) is presented in Fig. 4, indicating a finite temperature phase transition at $\beta_c \approx 7.0$.

This striped phase, with $\mathbf{q}_{cdw} = (0, \pi) \neq 2\mathbf{k}_F$, provides an explicit and quantitative illustration of a non-Peierls CDW instability. Recent experiments have exposed a similar behavior in a variety of materials, i.e., a charge order arising away from $2\mathbf{k}_F$ and whose origin cannot be related to FSN, such as in the quasi-2D materials NbSe$_2$, CeTe$_3$, Cr, and U and also in one-dimensional model systems like Au/Ge(001) [2,7,36–39]. In particular, NbSe$_2$ does not exhibit FSN or any divergence in the electronic susceptibility [8] nor a metal-insulator transition. Nevertheless, CDW order sets in at $T_{cdw} = 33.5$ K. The appearance of this phase, outside the usual Peierls paradigm, is then instead ascribed to strong EPC [2,3]. As noted earlier, the RPA criterion for CDW order suggests an intimate connection between momentum-dependent $g_{\mathbf{q}}$ and phonon dispersion $\omega(\mathbf{q})$, so that the results in Fig. 4 provide a confirmation that additional momentum structure plays a crucial role in the CDW ordering wave vector. In Supplemental Material [17], we discuss possible differences between $g_{\mathbf{q}}$ and $\omega(\mathbf{q})$, which lend some additional complexity.

Effect of dispersion on pairing.—We now turn to SC order. As noted earlier, it is uncommon for ODLRO to appear in fermionic models at half filling on bipartite geometries like the square lattice, which instead favor diagonal order. Nevertheless, the data in Fig. 2 show a rise in β_c with the increased energetic cost for (π, π)-CDW formation from the upward phonon dispersion. A natural
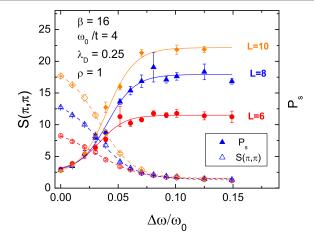

FIG. 5. The CDW-SC transition at half filling: As $\Delta\omega/\omega_0$ increases, $S(\pi, \pi)$ is strongly suppressed, while pairing susceptibility P_s is enhanced. Both quantities are in the same scale. Circles, triangles, and diamonds correspond to $L = 6, 8$, and 10, respectively. The filled (open) symbols represent P_s [$S(\pi, \pi)$]. The lines are just a guide to the eye.

question is whether that cost eventually becomes prohibitive, opening the door to SC.

To address this, we increase the SC scale of energy [40] and consider a phonon frequency $\omega_0/t = 4$, working with an upward phonon dispersion, as displayed in Fig. 1(c). For this frequency, the dispersionless HM ($\omega_2 = 0$) exhibits $T_{cdw} \sim 1/13$, without SC; see Supplemental Material [17]. However, for the dispersive case, $S(\pi, \pi)$ is strongly suppressed at $\Delta\omega/\omega_0 \gtrsim 0.05$, while P_s is enhanced and grows with lattice size, as displayed in Fig. 5, for fixed $\beta = 16$. That is, a CDW-SC transition should occur when $\Delta\omega/\omega_0$ increases. As presented in Fig. 6, at $\Delta\omega/\omega_0 = 0.10$, for instance, P_s grows with the lattice size for $\beta \gtrsim 12$. In order
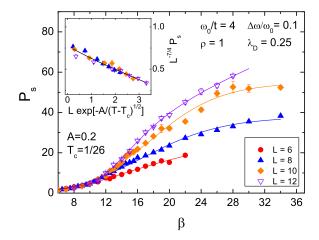

FIG. 6. *s*-wave pair susceptibility as a function of the inverse of temperature for $\Delta\omega/\omega_0 = 0.1$, $\omega_0/t = 4$, and $\lambda_D = 0.25$. Inset: The data collapse of the raw DQMC results by Kosterlitz-Thouless scaling for $\beta \geq 16$ (and $L = 8, 10$, and 12). The full lines are just a guide to the eye.

to establish quasi-long-range order for this case, the appropriate scaling ansatz is a Kosterlitz-Thouless (KT) behavior, $P_s = L^{2-\eta} f(L/\xi)$, with $\eta = 1/4$ and $\xi \sim \exp[A/(T - T_c)^{1/2}]$, $T \to T_c^+$. The inset in Fig. 6 displays the KT scaling of the P_s raw data for $\beta \geq 16$. Here, the parameters $A = 0.2$ and $T_c = 1/26$ yield the best data collapse. This result provides strong evidence for the onset of SC at half filling in the HM, when phonon dispersion is taken into account; see also Supplemental Material [17]. We should mention that recent results [41–48] have also examined the onset of SC in the HM, but they have not considered the effects of phonon dispersion. In the Holstein Hamiltonian, electron pairing is phonon induced, as described in the Eliasberg-Migdal theory [49,50].

Conclusions.—This Letter has provided a significant extension of QMC simulations of electron-phonon Hamiltonians by evaluating the effects of phonon dispersion on charge and pairing order in the Holstein model. The results offer several interesting features, including a CDW-SC transition at half filling and transitions between CDW phases at different ordering momenta, which can be tuned by a *weak* bare phonon dispersion. Our findings of a non-Peierls CDW phase, despite the existence of FSN in the bare electron dispersion, is of particular interest, given recent work questioning the traditional view of CDW formation [2,7,36–39]. In view of these, our results present further insight into the (complex) nature of CDW formation, exhibiting a new avenue to understand and, ultimately, to control it.

*natanael@if.ufrj.br, natanael.c.costa@gmail.com

[1] R. Peierls, *Quantum Theory of Solids* (Oxford University, New York, 1955).

[2] X. Zhu, Y. Cao, J. Zhang, E. Plummer, and J. Guo, Proc. Natl. Acad. Sci. U.S.A. **112**, 2367 (2015).

[3] X. Zhu, J. Guo, J. Zhang, and E. W. Plummer, Adv. Phys. X **2**, 622 (2017).

[4] A. Soumyanarayanan, M. Yee, Y. He, J. van Wezel, D. Rahn, K. Rossnagel, E. Hudson, M. Norman, and J. Hoffman, Proc. Natl. Acad. Sci. U.S.A. **110**, 1623 (2013).

[5] C. J. Arguello, S. P. Chockalingam, E. P. Rosenthal, L. Zhao, C. Gutiérrez, J. H. Kang, W. C. Chung, R. M. Fernandes, S. Jia, A. J. Millis, R. J. Cava, and A. N. Pasupathy, Phys. Rev. B **89**, 235115 (2014).

[6] F. Weber, S. Rosenkranz, J.-P. Castellan, R. Osborn, R. Hott, R. Heid, K.-P. Bohnen, T. Egami, A. H. Said, and D. Reznik, Phys. Rev. Lett. **107**, 107403 (2011).

[7] M. D. Johannes and I. I. Mazin, Phys. Rev. B **77**, 165135 (2008).

[8] M. D. Johannes, I. I. Mazin, and C. A. Howells, Phys. Rev. B **73**, 205102 (2006).

[9] M. Calandra, I. I. Mazin, and F. Mauri, Phys. Rev. B **80**, 241108 (2009).

[10] E. Da Silva Neto, P. Aynajian, A. Frano, R. Comin, E. Schierle, E. Weschke, A. Gyenis, J. Wen, J. Schneeloch, Z. Xu, S. Ono, G. Gu, M. Le Tacon, and A. Yazdani, Science **343**, 393 (2014).

[11] Q.-Y. Wang, Z. Li, W.-H. Zhang, Z.-C. Zhang, J.-S. Zhang, W. Li, H. Ding, Y.-B. Ou, P. Deng, K. Chang, J. Wen, C.-L. Song, K. He, J.-F. Jia, S.-H. Ji, Y.-Y. Wang, L.-L. Wang, X. Chen, X.-C. Ma, and Q.-K. Xue, Chin. Phys. Lett. **29**, 037402 (2012).

[12] R. Peng, H. Xu, S. Tan, H. Cao, M. Xia, X. P. Shen, Z. Huang, C. Wen, Q. Song, T. Zhang, B. Xie, X. Gong, and D. Feng, Nat. Commun. **5**, 5044 (2014).

[13] Y. Wang, K. Nakatsukasa, L. Rademaker, T. Berlijn, and S. Johnston, Supercond. Sci. Technol. **29**, 054009 (2016).

[14] S. Li, E. A. Nowadnick, and S. Johnston, Phys. Rev. B **92**, 064301 (2015).

[15] J. L. Raimbault and S. Aubry, J. Phys. Condens. Matter **7**, 8287 (1995).

[16] D. J. J. Marchand and M. Berciu, Phys. Rev. B **88**, 060301 (2013).

[17] See Supplemental Material at http://link.aps.org/supplemental/10.1103/PhysRevLett.120.187003 for more details about (i) electron-phonon interactions, (ii) DQMC method, (iii) data collapses, and (iv) density of states, which includes Refs. [18–26].

[18] R. Blankenbecler, D. J. Scalapino, and R. L. Sugar, Phys. Rev. D **24**, 2278 (1981).

[19] R. T. Scalettar, N. E. Bickers, and D. J. Scalapino, Phys. Rev. B **40**, 197 (1989).

[20] R. M. Noack, D. J. Scalapino, and R. T. Scalettar, Phys. Rev. Lett. **66**, 778 (1991).

[21] R. R. dos Santos, Braz. J. Phys. **33**, 36 (2003).

[22] M. Creutz and B. Freedman, Ann. Phys. (N.Y.) **132**, 427 (1981).

[23] R. T. Scalettar, R. M. Noack, and R. R. P. Singh, Phys. Rev. B **44**, 10502 (1991).

[24] M. Vekić, R. M. Noack, and S. R. White, Phys. Rev. B **46**, 271 (1992).

[25] M. Jarrell and J. Gubernatis, Phys. Rep. **269**, 133 (1996).

[26] G. G. Batrouni, R. T. Scalettar, G. T. Zimanyi, and A. P. Kampf, Phys. Rev. Lett. **74**, 2527 (1995).

[27] J. E. Hirsch and S. Tang, Phys. Rev. Lett. **62**, 591 (1989).

[28] S. R. White, D. J. Scalapino, R. L. Sugar, E. Y. Loh, J. E. Gubernatis, and R. T. Scalettar, Phys. Rev. B **40**, 506 (1989).

[29] H. Q. Lin and J. E. Hirsch, Phys. Rev. B **35**, 3359 (1987).

[30] T. Holstein, Ann. Phys. (N.Y.) **8**, 325 (1959).

[31] Since unequal-time measurements are more time consuming, our analyses of susceptibilities are restricted to pairing: The appearance of SC in 2D lattices occurs as a quasi-long-range-order transition, requiring stronger signals to be identified.

[32] N. C. Costa, W. Hu, Z. J. Bai, R. T. Scalettar, and R. R. P. Singh, Phys. Rev. B **96**, 195138 (2017).

[33] M. Weber and M. Hohenadler, arXiv:1709.01096.

[34] C. Chen, X. Y. Xu, J. Liu, G. Batrouni, R. Scalettar, and Z. Y. Meng, arXiv:1802.06177.

[35] These results also agree with the max. entropy method; see Supplemental Material [17].

[36] M. Maschek, S. Rosenkranz, R. Heid, A. H. Said, P. Giraldo-Gallo, I. R. Fisher, and F. Weber, Phys. Rev. B **91**, 235146 (2015).

[37] D. Lamago, M. Hoesch, M. Krisch, R. Heid, K.-P. Bohnen, P. Böni, and D. Reznik, Phys. Rev. B **82**, 195121 (2010).

[38] S. Raymond, J. Bouchet, G. H. Lander, M. Le Tacon, G. Garbarino, M. Hoesch, J.-P. Rueff, M. Krisch, J. C. Lashley, R. K. Schulze, and R. C. Albers, Phys. Rev. Lett. **107**, 136401 (2011).

[39] C. Blumenstein, J. Schäfer, M. Morresi, S. Mietke, R. Matzdorf, and R. Claessen, Phys. Rev. Lett. **107**, 165702 (2011).

[40] In the Bardeen-Cooper-Schrieffer theory, $T_c \sim \omega_D e^{-[1/V_0 N(E_F)]}$, with ω_D being the Debye frequency. For optical phonons with a small phonon bandwidth, one can roughly assume $\omega_D = \omega_0$ and $V_0 \sim W \lambda_D$.

[41] H. Bakrim and C. Bourbonnais, Europhys. Lett. **90**, 27001 (2010).

[42] H. Bakrim and C. Bourbonnais, Phys. Rev. B **91**, 085114 (2015).

[43] C. Lin, B. Wang, and K. H. Teo, Phys. Rev. B **93**, 224501 (2016).

[44] C. Lin, B. Wang, and K. H. Teo, Physica (Amsterdam) **532C**, 27 (2017).

[45] C. B. Mendl, E. A. Nowadnick, E. W. Huang, S. Johnston, B. Moritz, and T. P. Devereaux, Phys. Rev. B **96**, 205141 (2017).

[46] I. Esterlis, B. Nosarzewski, E. W. Huang, B. Moritz, T. P. Devereaux, D. J. Scalapino, and S. A. Kivelson, Phys. Rev. B **97**, 140501(R) (2018).

[47] T. Ohgoe and M. Imada, Phys. Rev. Lett. **119**, 197001 (2017).

[48] S. Karakuzu, L. F. Tocchio, S. Sorella, and F. Becca, Phys. Rev. B **96**, 205145 (2017).

[49] A. Migdal, Sov. Phys. JETP **7**, 996 (1958).

[50] G. Eliashberg, Sov. Phys. JETP **11**, 696 (1960).